Received June 29, 2018, accepted August 8, 2018, date of publication August 21, 2018, date of current version September 21, 2018.

Digital Object Identifier 10.1109/ACCESS.2018.2866506

Mine Water Inrush Sources Online Discrimination Model Using Fluorescence Spectrum and CNN

YONG YANG[1,2], JIANHUA YUE[1], JING LI[3], AND ZHONG YANG[4]
[1]School of Resources and Geosciences, China University of Mining and Technology, Xuzhou 221008, China
[2]School of Information and Electrical Engineering, Xuzhou College of Industrial Technology, Xuzhou 221104, China
[3]School of Information Engineering, Nanjing Audit University, Nanjing 211815, China
[4]School of Intelligence Science and Control Engineering, Jinling Institute of Technology, Nanjing 211100, China

Corresponding author: Jianhua Yue (yuejh@cumt.edu.cn)

This work was supported in part by the Twelfth Five Year National Science and Technology Support Program under Grant 2013BAK06B01, in part by the National Nature Science Foundation of China under Grant 41674133, Grant 61673108, and Grant 51875100, in part by the Nature Science Foundation of Xingjian Uighur Autonomous Region under Grant 2016D01C067, in part by the Ministry of Education Cooperation in Industry and Education under Grant 201602009006, and in part by the Innovation Project of Jiangsu Province.

ABSTRACT Mine water inrush disasters served as severe accidents in China cause severe economic losses and threaten the safety of coal mine production. The existing mine water sources discrimination methods have to let miners collect water samples of different place *in situ*, which make dynamic online analysis virtually impossible. This paper proposes a novel inrush water source discrimination model using laser-induced fluorescence (LIF) technology and convolution neural network (CNN) to achieve mines inrush water source online discrimination which can reduce humankind involvement. Experiment collected 161 items water samples of four different water sources of Xinji No. 2 coal mine. The LIF auto launched 405-nm lasers into water samples to calculate reflected fluorescence spectra. An improved smoothing method is proposed to reduce high-frequency random fluctuations of fluorescence spectra and further to compute auto-correlation fluorescence spectra features. Based on CNN frame and spectra features, mine waters source online discrimination model is constructed. Experiment randomly selected 80 percent of samples of all for training CNN model, the remaining for testing the proposed model. Theoretical analysis and experimental results demonstrate that the recognition rate of the proposed method achieves 98%.This method is an effective assessment method to discriminate inrush water source types of mines. It provides a new train of thought to solve online discriminant inrush water source types of mines.

INDEX TERMS Fluorescence spectra, CNN, mine inrush, water source discrimination.

I. INTRODUCTION

Water inrush disasters in mines served as serious accidents in China have engendered severe economic losses [1]. With the increasing depths of mining, hydrogeological conditions including crustal stress and water inflow and so on are much more complex. Also aquiclude of coal seam floor faced risks of destruction by mining. Above factors pose grave threats to security in China mine production.

Many researches have demonstrated that different water sources in different aquifers have distinctive hydrochemical and physical characteristics. Thus, finding these characteristics is an effective way to identify mine inrush water source types, further to analyze principal component of water body and find water flow conditions for effectively and accurately forecasting mine water inrush disaster.

Now available mine water source discrimination methods include trace elements [2], representative ion [3], water temperature level [4] and Geographic Information System (GIS). Several different parameters have been widely used and achieved excellent results, but water samples must be collected by miners from several in situ for measurement in the ground. Apparent disadvantages, including heavy workloads, much consumption of time and samples susceptible to contamination, make dynamic measurement virtually impossible. Wang *et al.* [5] proposed LIF technology to measure the fluorescence spectrum of water inrush water sources in mines, which cannot contaminate water source any more. Experimental results reveal that Fluorescence spectra have excellent ability to grasp formation and evolution of water channel. These characteristics served as crucial foundation of scientific decision are used to predict coal mine water inrush disaster.

Excellent Discriminant model is the other key factor to predict water inrush disaster accurately. Sun and Gui [6] uses Support Vector Machine (SVM) to identify mine water inrush multi-source discrimination. Qiang *et al.* [7] presented system clustering analysis method to identify different types of coal mine water. Zhao *et al.* [8] adopted Extreme Learning Machine (ELM) algorithm to construct a multiple classification model for mine waters inrush disaster forecasting. However, all above traditional neural networks have trapped by shallow frameworks limitations. For example, amounts of prior knowledge achieved from various experts are necessary to select effective features. Features are subjective and incomplete [9]–[11]. Second, if objective function of multi-layer BP network is non-convex, the initial weights selected randomly in training process, the model was likely to be trapped in a local optimal value.

Deep learning has been proposed based on the framework of Deep Neural Network (DNN). It has excellent characteristics of neuron numbers and Network depth to simulate almost any continuous function. DNN using multi layers framework can express feature effectively and objectively than shallow networks [1], [19], [20]. Convolutional Neural Network (CNN) served as a crucial deep learning method directly adopts two-dimensional image data mapped into the model to avoid complex feature extraction computation and humankind subjective feature selection. Besides, convolution and pooling computation, samples processed by shift, tilting and scaling still keep stable [12]–[15].

This paper proposes a novel mine water inrush source type online discrimination model using LIF technology and CNN. First, water inrush fluorescence spectra are recorded by LIF technology to improve the real-time and reduce water samples chemical contamination. Second, an improved filtering method is presented to compute auto-correlation fluorescence spectra in two-dimensional space, which is further to reduce high-frequency random fluctuations of fluorescence spectra and enhance characteristics of different water sources for discrimination analysis. Third, combined with image features and deep learning model, discrimination model based on deep Convolutional Neural Network is proposed to auto discriminate water inrush source online using auto-correlation spectra to avoid feature selection in a subjective way. By comparison with traditional measurement methods, experiment results illustrate that the correct recognition rate of water sources approaches 98%. This improved filtering method can effectively suppress the fluorescent noise and enhance characteristics of different types of water sources. It is an effective method to discriminate mine water inrush sources online.

II. MATERIALS AND METHODS

A. EQUIPMENT

Experiment adopted the LIFS-405 laser-induced fluorescence system produced by Guangdong Biao Qi Electronics Co. Ltd. The fixed laser incident wavelength is 405 nm, the incident laser power is 120 mW, spectral scanning step is 0.5 nm and spectral scanning time is 0.001 s/nm.

B. EXPERIMENTAL MATERIALS AND SPECTRAL DATA ACQUISITION

Water samples used in the paper are collected from the No. 2 Xinji coal mine of Huainan Mining Group. Water samples were collected in batches from June 2016 to June 2017, which included 46 items from the goaf hydrops, 59 items from Sandstone water, 42 items from Limestone water and 14 items from Ordovician Limestone water. All collected samples were placed in airtight polypropylene sample bottles, which had been washed by 10% HCL and distilled water before. Fluorescence spectra of water samples were measured by LIF equipment as soon as possible. Considering the influence of background light and human behavior, the experiment should be carried out in a dark environment. The received spectrum range of the monitor computer is 340-1340 nm with 0.5nm wavelength resolutions. The spectrum data corresponding to each item is 2048 dimensions. To ensure the accuracy of the test and reduce the random error caused by external interference, each sample was measured 10 times to calculate their arithmetic mean value. The spectral curves of the water sample are shown in Fig. 1. Principal spectrum energy is concentrated on 420nm∼720nm. The rest wavelength parts of four different water sources were almost indiscernible.

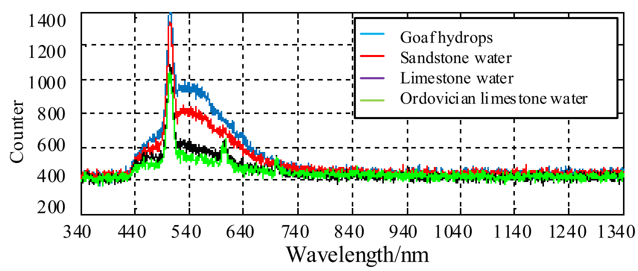

FIGURE 1. **Fluorescence spectra.**

C. PRINCIPAL COMPONENT ANALYSIS OF FLUORESCENCE SPECTRA

All Fluorescence Spectra items are processed using the principal component analysis (PCA) method. According to different PCA dimension, the cumulative contribution rates of extracted principal components are shown in Table 1. Variance eigenvalues of the first three principal components are all exceeding 1. It indicates that the first three principal components are important to discriminate different types of water sources. However, cumulative contribution rate of the first 10 principal components is merely 80.94%, below the 85% criterion [16]. It indicates that ten principal components are not enough to accurately discriminate different types of water source.

TABLE 1. Principal component contributor rate.

Principal Component	Variance	Accumulative Contribution Rate %
PC1	53.13	53.13
PC2	21.44	74.58
PC3	2.69	77.27
PC4	0.76	78.03
PC5	0.58	78.62
PC6	0.48	79.11
PC7	0.47	79.58
PC8	0.46	80.05
PC9	0.45	80.50
PC10	0.43	80.94

It set the first, second and third principal components (PC1, PC2 and PC3) as X, Y and Z coordinates respectively to describe distinguish ability of four types of water sources in Fig. 2. It can be seen that all four of these water sources have no obvious boundary to discriminate. The PCA method is insufficient to identify these four different water sources accurately.

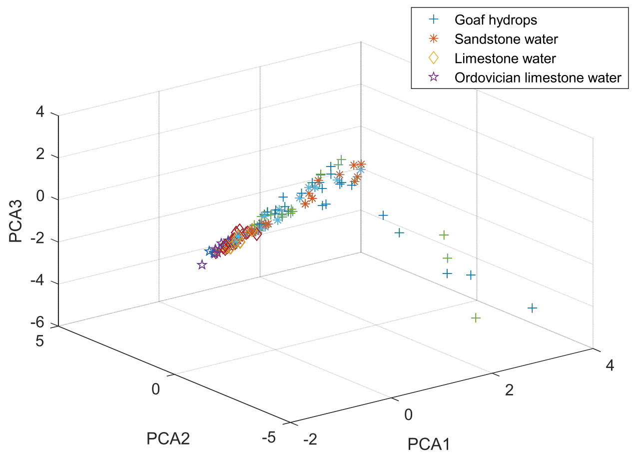

FIGURE 2. Principal component scores scatter plot(PC1×PC2×PC3).

D. AN IMPROVED RECURSIVE MEAN FIRST-ORDER LAG FILTER METHOD

Fig 1 presents the Fluorescence spectra using LIF technology. All these curves show high-frequency fluctuation interference, which is not conducive to the identification of water sources. Among the smoothing filter processing algorithms, the recursive average method provides a fast computation efficiency to satisfy online discriminant. The first-order lag filter method decreases the periodic interference in high-frequency fluctuation conditions. Based on these two methods, the paper proposes a new filtering algorithm to process fluctuation interference in fluorescent spectra. The recorded spectral data is first processed by first-order filtering method as shown in the following:

$$y = y_2 \times (1 - a) + a \times y_1 \tag{1}$$

where y is the output of the spectral filter and y_2 is the fluorescence spectrum amplitude. y_1 is the first-order lag wavelength of y_2. a is the weight between present wavelength and last wavelength. Then, using the recursive average method, N samples are viewed as one sequence to calculate the arithmetic mean value.

E. CLASSIFICATION MODEL OF MINE WATER INRUSH SOURCE BASED ON CNN

Fig. 3 presents the CNN structure, including the input layer, hidden layer, full connection layer and output layer. The hidden layer defines several convolution layers and the pooling layers connecting alternately. The convolution layer adopts various specific convolution kernels, biases and an activation function to compute output features. The pooling layer is the selection process of output features using the mean pool and the maximum pool. The fully connected layer and the output layer constitute the classifier, which can be Logistic Regression, Softmax Regression and SVM. Because Softmax Regression model is a multi-class extension of a Logistic Regression to solve multiple classification problems, Softmax Regression is selected as a classifier in this paper.

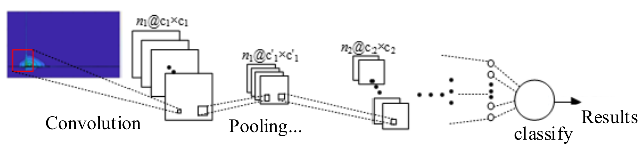

FIGURE 3. CNN structure.

The CNN model was a supervised learning process.In training model process, forward propagation and back propagation are discussed respectively as follows:

1) FORWARD PROPAGATION

In CNN model, forward propagation begins with a number of hidden layers alternating with convolution and pooling. Next to the output layer, all of the two-dimensional features are converted into one-dimensional features mapped into a fully connected layer. Then, the full connection is used to transmit one-dimensional features to the Softmax classifier for the recognition results.

Suppose there are m input train samples ($\mathbf{X} = [\boldsymbol{x}^{(1)}, \boldsymbol{x}^{(2)}, \ldots, \boldsymbol{x}^{(m)}]$, $x^{(i)} \in \Re^{n+1}$, $i = 1, 2, \ldots, m$), where m is the number of input samples, and $x^{(i)}$ is defined in $n+1$ dimensional Euclidean space. The corresponding label is $\mathbf{Y} = [y^{(1)}, y^{(2)} \ldots y^{(m)}]$. If there are K classifications, the value of $y(i)$ will be between 1 to K. For a Softmax model whose sample is $\boldsymbol{x}^{(i)}$ and parameter vector is $\boldsymbol{\theta}$, the softmax outputs $p(y^{(i)} = 1 \,|\, x^{(i)}; \boldsymbol{\theta}), \ldots, p(y^{(i)} = K \,|\, x^{(i)}; \boldsymbol{\theta})$ are occurrence probabilities of each classification. The $h_{\boldsymbol{\theta}}(x^{(i)})$ is occurrence probabilities set of i-th sample and parameter $\boldsymbol{\theta}$.

$$h_{\boldsymbol{\theta}}(x^{(i)}) = \begin{bmatrix} p(y^{(i)}=1 \,|\, x^{(i)};\boldsymbol{\theta}) \\ p(y^{(i)}=2 \,|\, x^{(i)};\boldsymbol{\theta}) \\ \vdots \\ p(y^{(i)}=K \,|\, x^{(i)};\boldsymbol{\theta}) \end{bmatrix} = \frac{1}{\sum_{k=1}^{K} e^{\boldsymbol{\theta}_k^T x^{(i)}}} \begin{bmatrix} e^{\boldsymbol{\theta}_1^T x^{(i)}} \\ e^{\boldsymbol{\theta}_2^T x^{(i)}} \\ \vdots \\ e^{\boldsymbol{\theta}_K^T x^{(i)}} \end{bmatrix} \tag{2}$$

$\boldsymbol{\theta}_k$ is the parameter vector of the k-th label. The denominator is the normalization of probability distribution. k. $y_k^{(i)}$ is the probability of sample $x^{(i)}$ belonging to classification Suppose that $t_k^{(i)}$ is the probability of sample $x^{(i)}$ belonging to classification k predicted by model. Then, the real and theoretical label distribution of the model can be validated by cross-entropy, as shown in following:

$$L = -\sum_{i=1}^{m}\sum_{k=1}^{K} t_k^{(i)} \log(y_k^{(i)}) \tag{3}$$

Then, the cost function of Softmax model is obtained as follows:

$$J(\boldsymbol{\theta}) = -\frac{1}{m}[\sum_{i=1}^{m}\sum_{k=1}^{K} 1\{y^{(i)}=k\} \log \frac{e^{\boldsymbol{\theta}_j^T x^{(i)}}}{\sum_{l=1}^{K} e^{\boldsymbol{\theta}_l^T x^{(i)}}}] \tag{4}$$

In practical applications, the loss function of the Softmax Regression model is not strictly non-convex, and the optimal solution to the calculated parameters is not unique. To avoid this problem, it often modifies the cost function by adding a weight decay term to solve redundant set of parameters problems of the Softmax Regression. In the corresponding formula, the weight attenuation coefficient is assumed as λ; then, the cost function corresponding to the Softmax is as follows:

$$J(\boldsymbol{\theta}) = -\frac{1}{m}[\sum_{i=1}^{m}\sum_{k=1}^{K} 1\{y^{(i)}=k\} \log \frac{e^{\boldsymbol{\theta}_j^T x^{(i)}}}{\sum_{l=1}^{K} e^{\boldsymbol{\theta}_l^T x^{(i)}}}] + \frac{\lambda}{2}\sum_{i=1}^{K}\sum_{j=0}^{n} \boldsymbol{\theta}_{ij}^2 \tag{5}$$

2) BACK PROPAGATION

To compute the optimal parameters of the CNN model, the gradient descent method is used to update the parameter vector:

$$\nabla_{\boldsymbol{\theta}_j} J(\boldsymbol{\theta}) = -\frac{1}{m}[\sum_{i=1}^{m} x^{(i)}(1\{y^{(i)}=k\} - p(y^{(i)}=j \,|\, x^{(i)};\boldsymbol{\theta}))] + \lambda\boldsymbol{\theta}_j \tag{6}$$

where $\boldsymbol{\theta}$ is a matrix composed of all parameters. Update the components of each line of $\boldsymbol{\theta}$ one by one to obtain the updated values of all the parameters.

$$\boldsymbol{\theta} = \begin{bmatrix} \boldsymbol{\theta}_1^T \\ \boldsymbol{\theta}_2^T \\ \cdots \\ \boldsymbol{\theta}_K^T \end{bmatrix} \tag{7}$$

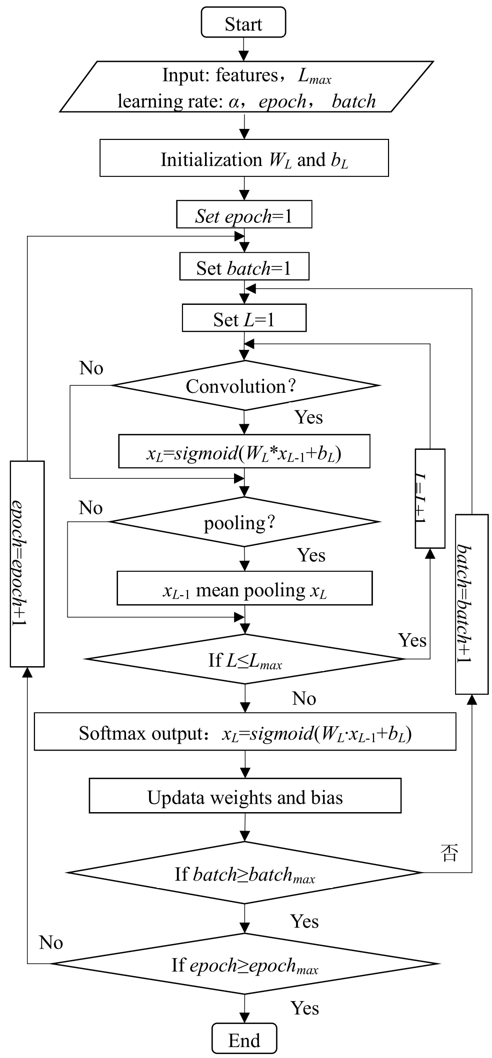

FIGURE 4. Training process of CNN.

The Softmax Regression model is obtained by minimizing the $J(\boldsymbol{\theta})$. Fig. 4 shows training process of CNN model. First, the training parameters, the network weights and bias initialization should be set. After processed by the hidden layers and the fully connected layer, the input features are transmitted to the output layer. Then, the error between the actual and expected output propagates layer-by-layer using BP back-propagation algorithm, which is assigned to each layer to adjust the network weights and bias until meeting the convergence condition.

III. EXPERIMENT AND RESULT ANALYSIS

A. AN IMPROVED RECURSIVE MEAN FIRST-ORDER LAG FILTER METHOD

Fig. 5 presents pre-processing results using the proposed filtering algorithm, where parameters $a = 0.5$ and $N = 14$. These four curves respond with relatively ideal smoothing effects. Curves peaks are also obvious variation at the same time.

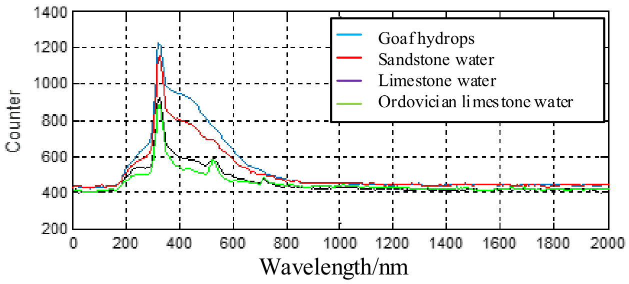

FIGURE 5. First-order lag and recursive average filtering results.

Fig. 6 presents auto-correlation fluorescence spectra using the proposed method based on four different kinds of water samples, including goaf hydrops, Sandstone water, Limestone water and Ordovician Limestone water. There are obvious differences among auto-correlation spectra. Within the range of the wavelength, goaf hydrops excited by 405 nm lasers, shows 7 levels of energy intensity. The energy is distributed over a wide range of wavelengths and shows a tendency to diverge gradually, which is consistent with increased organic compounds in water. Sandstone water excited by 405 nm lasers, shows 6 levels of energy intensity. The energy is distributed in a wide range of wavelengths, and the lowest 3 levels show a tendency to diverge gradually, which is consistent with reduced organic compounds in water. Limestone water, excited by 405 nm lasers, shows 6 levels of energy intensity. The energy is also distributed over a wide range of wavelengths, and the lowest 2 levels show a tendency to diverge gradually, which is consistent with further reduced organic compounds in the water. Ordovician Limestone water was excited by 405 nm lasers, which displays 6 levels of energy intensity. The energy is especially distributed over a narrow range of wavelengths, and it shows an obvious tendency toward convergence, which is consistent with fewer organic compounds in clear water. These results conclude that the proposed method achieves a clear discrimination between Sandstone water and Limestone water and displays obvious convergence in the Ordovician Limestone water, with little noise at 580 nm. It is shown that the improved filtering algorithm performs well at de-noising the data and feature discrimination. Fig. 7 and Fig. 8 present auto-correlation fluorescence spectra using a recursive average and first-order lag filter method. Based on 4 different water samples, auto-correlation spectra using recursive average filtering method appear more obvious distinction than First-order lag filtering method. Auto-correlation spectra using First-order lag filtering method show clear divergence tendency. However, combined with the proposed First-order lag and recursive average filtering method, the proposed method is the optimal conducive to the further analysis of the spectral curve.

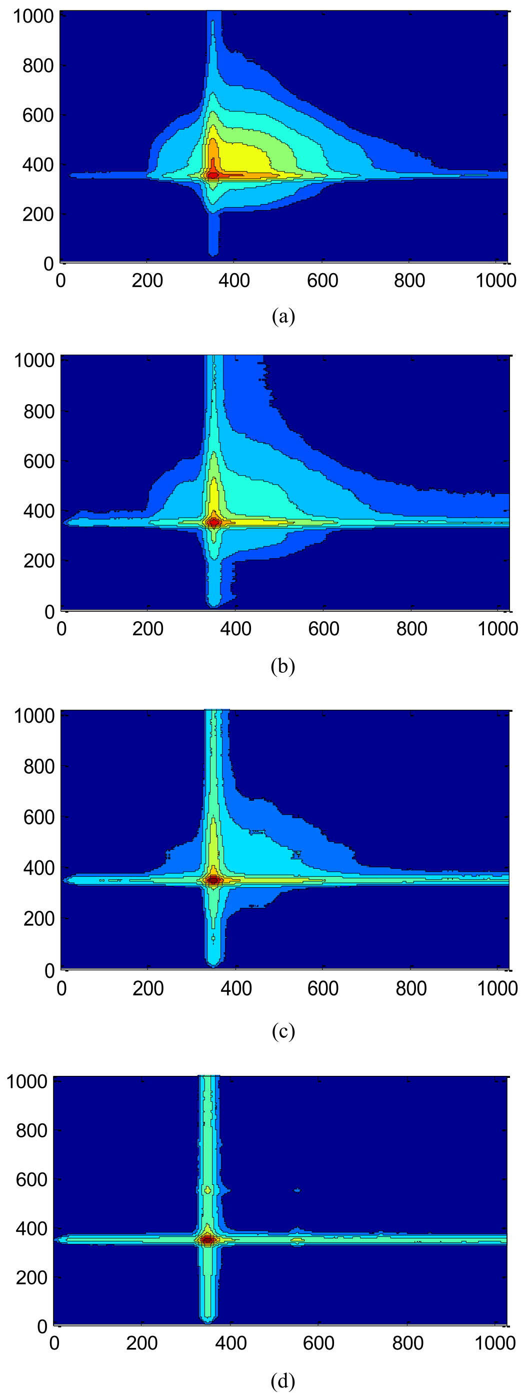

FIGURE 6. First-order lag and recursive average filtering auto-correlation spectra. (a) Goaf hydrops. (b) Sandstone water. (c) Limestone water. (d) Ordovician Limestone water.

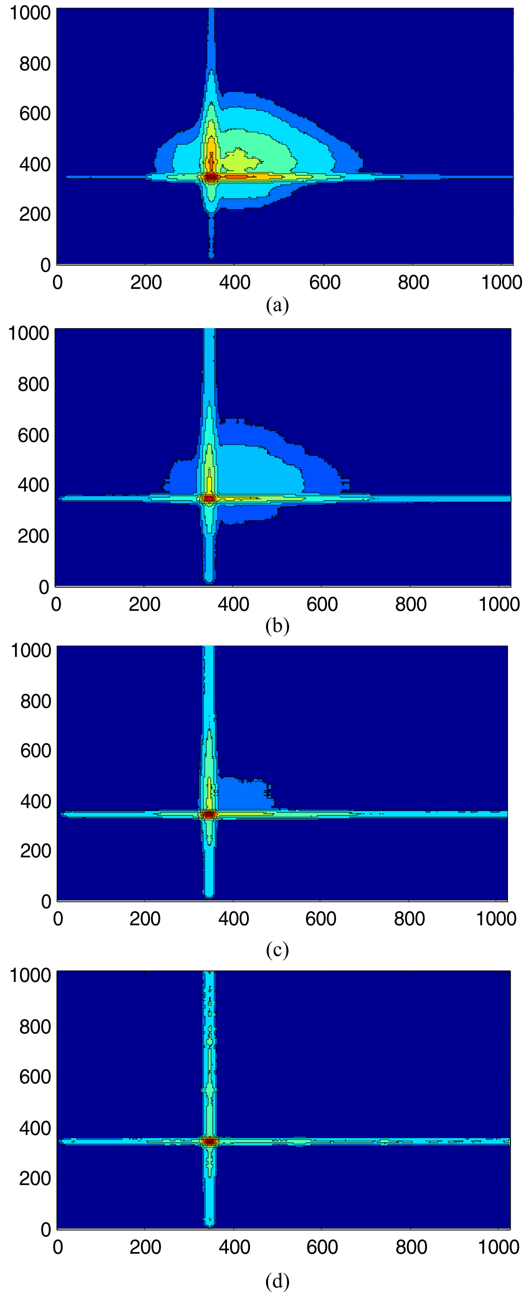

FIGURE 7. **Recursive average filtering auto-correlation spectra. (a) Goaf hydrops. (b) Sandstone water. (c) Limestone water. (d) Ordovician Limestone water.**

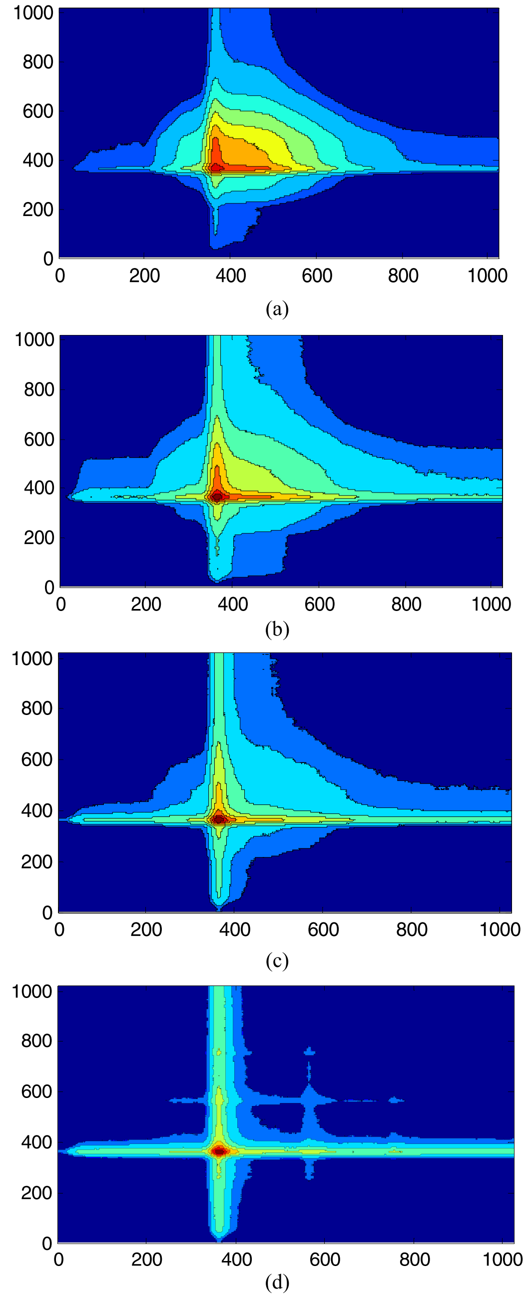

FIGURE 8. **First-order lag filtering auto-correlation spectra. (a) Goaf hydrops. (b) Sandstone water. (c) Limestone water. (d) Ordovician Limestone water.**

IV. EXPERIMENT AND RESULT ANALYSIS

A. CNN MODEL EXPERIMENT AND RESULT ANALYSIS

This experiment verifies discriminant performance on four types of test water samples, including goaf hydrops, Sandstone water, Limestone water and Ordovician Limestone water. Auto-correlation spectra are obtained by using auto-correlation and normalization of one-dimensional spectral data. It adopts 5-fold cross-validation; 20% random samples used for the test and the remaining 80% used to train the CNN model. The CNN model, as shown in Fig. 1, is constructed by convolution, pooling layer, convolution, pooling layer, convolution, pooling layer, full connection layer, and classifier. The first convolution layer adopts the convolution kernel 64@256×256. The convolution kernel of the second convolution layer is 128@64×64. The third convolution layer adopts convolution kernel 192@16×16. The pooling layer is mean pool with size 2×2. Training parameters of the network are set as shown in Table 2.

Fig. 9 presents discrimination results using mentioned three filter methods and the CNN model. Red lines show

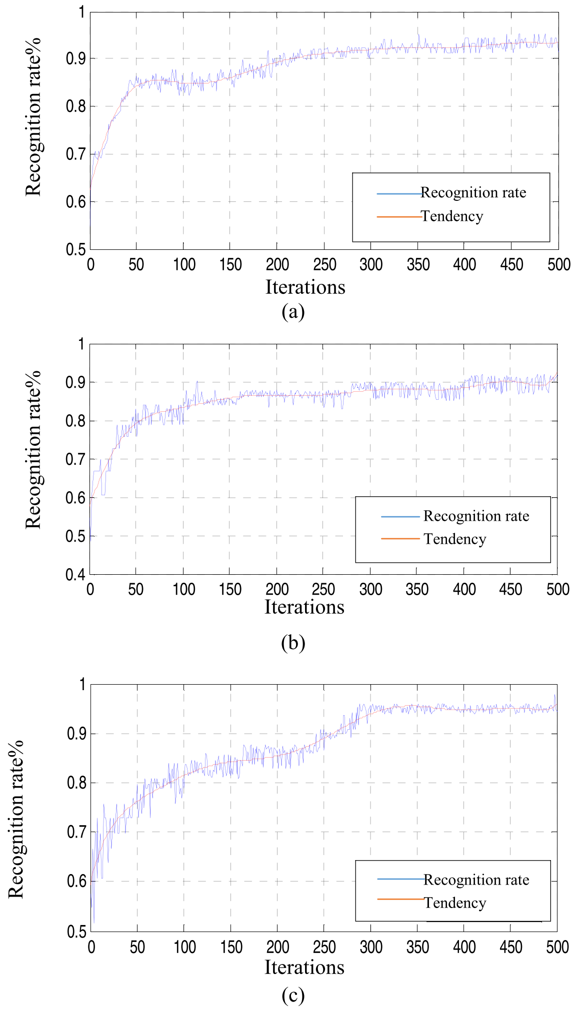

FIGURE 9. Recognition results of 3 filter methods. (a) Recursive average filtering. (b) First-order lag filtering. (c) First-order lag and recursive average filtering.

TABLE 2. Parameters setting.

Parameter	Value
Hyper parameters	Values
Dropout ratio	0.2
Moment	0.9
Learn rate	0.0025
Regularization type	L_2
Minibatch	64

a gradually increasing tendency of correct recognition with iterations increasing. The proposed method shows a gradually increasing tendency of correct recognition as iterations increase. The average recognition rate reached 87.56%, the average recognition rate after stabilization reached 94.95%, and the highest recognition rate reached 98%. The results show that the first-order lag and recursive average filtering auto-correlation spectra can decrease the fluorescence noise and highlight characteristics of the water source in a different aquifer.

Considering the mine water inrush source discrimination accuracy using different models, this experiment makes a comparison between the proposed method and the PCA-BP model [7], [8]. The BP model parameters are set as a three-layer network model and Tansig activation function. First, the PCA was carried out on the spectral data processing. The PCA dimensions are set to 3, 4, 6, and 8. Then, all samples are set as training datasets. The experiment randomly selects samples that are set as test datasets to determine the effect of the BP model. The types of water source are marked as follows: 1 is water in Goaf hydrops, 2 is Sandstone water, 3 is Limestone water and 4 is Ordovician Limestone water.

TABLE 3. Recognition rate of PCA-BP algorithm.

	PCA=3	PCA=4	PCA=6	PCA=8
1	90	85	80	60
2	75	90	80	70
3	80	80	85	75
4	90	85	75	70
Recognition rate	83.75	85	80	68.75

Table 3 shows that when the number of principal components was set as 4, the recognition rate approaches 85%. When the number of principal components was set to 8, the recognition rate is reduced up to 68.75%. It can be seen that this mine water inrush sources online discrimination using CNN and fluorescence spectra performs with higher accuracy than using traditional PCA-BP model.

V. CONCLUSIONS

This paper proposes a novel inrush water sources discrimination model using LIF and CNN to solve mine water sources online discrimination. The proposed method was further applied to 4 types of water source discriminant analyses. The characteristics of the proposed method include the following: an improved smoothing method to compute auto-correlation fluorescence spectra for high-frequency random fluctuation suppression and feature difference enhancement, and water source discriminant model based on the CNN frame using auto-correlation spectra to avoid feature selection in a subjective way. The theoretical analysis and experimental results show that the proposed method is an effective assessment method to define inrush water source types in a mine. It provides a new method to solve online discrimination of inrush water sources in mines.

VI. CONFLICT OF INTEREST

The authors declare that there are no conflicts of interest regarding the publication of this paper.

REFERENCES

[1] L. H. Sun, "Statistical analysis of hydrochemistry of groundwater and its implications for water source identification: A case study," *Arabian J. Geosci.*, vol. 7, no. 9, pp. 3417–3425, 2014.

[2] J. Wu, F.-P. Cui, S.-Q. Zhao, S.-J. Liu, Y.-F. Ceng, and Y.-W. Gu, "Type classification and main characteristics of mine water disasters," *J. China Coal Soc.*, vol. 38, no. 4, pp. 561–565, 2013.

[3] G. Li, X. Wang, Z. Meng, and H. Zhao, "Seawater inrush assessment based on hydrochemical analysis enhanced by hierarchy clustering in an undersea goldmine pit, China," *Environ. Earth Sci.*, vol. 71, no. 12, pp. 4977–4987, 2014.

[4] Z. Meng, G. Li, and X. Xie, "A geological assessment method of floor water inrush risk and its application," *Eng. Geol.*, vols. 143–144, pp. 51–60, Aug. 2012.

[5] Q. Wang, X. Wang, and Q. Hou, "Geothermal water at a coal mine: From risk to resource," *Mine Water Environ.*, vol. 35, no. 3, pp. 294–301, 2016.

[6] L. Sun and H. Gui, "Hydro-chemical evolution of groundwater and mixing between aquifers: A statistical approach based on major ions," *Appl. Water Sci.*, vol. 5, no. 1, pp. 97–104, 2015.

[7] W. Qiang, L. Bo, and C. Yulong, "Vulnerability assessment of groundwater inrush from underlying aquifers based on variable weight model and its application," *Water Resour. Manage.*, vol. 30, no. 10, pp. 3331–3345, 2016.

[8] Z. Zhao, P. Li, and X. Xu, "Forecasting model of coal mine water inrush based on extreme learning machine," *Appl. Math. Inf. Sci.*, vol. 7, no. 3, pp. 1243–1250, 2013.

[9] F. Gong, Z. Fu, and J. Lu, "Headstream identification of mine water-inrush source based on multivariate discriminant analysis method," *Disaster Adv.*, vol. 6, no. 6, pp. 444–450, 2013.

[10] W. Bing-Qiang *et al.*, "Prediction of mine water inrush sources based on cluster analysis of hydrogeo chemical features," *J. Hebei Univ. Eng. (Natural Sci. Ed.)*, vol. 3, no. 3, p. 25, 2015.

[11] J. Qian, L. Wang, L. Ma, Y. Lu, W. Zhao, and Y. Zhang, "Multivariate statistical analysis of water chemistry in evaluating groundwater geochemical evolution and aquifer connectivity near a large coal mine, Anhui, China," *Environ. Earth Sci.*, vol. 75, p. 747, May 2016.

[12] I. Matiatos, A. Alexopoulos, and A. Godelitsas, "Multivariate statistical analysis of the hydrogeochemical and isotopic composition of the groundwater resources in northeastern Peloponnesus (Greece)," *Sci. Total Environ.*, vols. 476–477, pp. 577–590, Apr. 2014.

[13] X. Ni, P. H. S. W. Kulatilake, Z. Chen, P. Gong, and H. Kong, "Experimental investigation of non-darcy flow in sandstone," *Geotechn. Geol. Eng.*, vol. 34, no. 6, pp. 1835–1846, Dec. 2016.

[14] D. Ma and H. Bai, "Groundwater inflow prediction model of karst collapse pillar: A case study for mining-induced groundwater inrush risk," *Natural Hazards*, vol. 76, no. 2, pp. 1319–1334, 2015.

[15] L. Chen, X. Feng, W. Xie, and D. Xu, "Prediction of water-inrush risk areas in process of mining under the unconsolidated and confined aquifer: A case study from the Qidong coal mine in China," *Environ. Earth Sci.*, vol. 75, p. 706, Apr. 2016.

[16] W. Yang, X. Xia, B. Pan, C. Gu, and J. Yue, "The fuzzy comprehensive evaluation of water and sand inrush risk during underground mining," *J. Intell. Fuzzy Syst.*, vol. 30, no. 4, pp. 2289–2295, 2016.

[17] Y. Wang, W. Yang, M. Li, and X. Liu, "Risk assessment of floor water inrush in coal mines based on secondary fuzzy comprehensive evaluation," *Int. J. Rock Mech. Mining Sci.*, vol. 52, pp. 50–55, Jun. 2012.

[18] Y. Zeng, Q. Wu, S. Liu, Y. Zhai, W. Zhang, and Y. Liu, "Vulnerability assessment of water bursting from Ordovician limestone into coal mines of China," *Environ. Earth Sci.*, vol. 75, no. 22, p. 1431, 2016.

[19] X. X. Zhu *et al.*, "Deep learning in remote sensing: A comprehensive review and list of resources," *IEEE Geosci. Remote Sens. Mag.*, vol. 5, no. 4, pp. 8–36, Dec. 2018.

[20] N. Akhtar and A. Mian, "Threat of adversarial attacks on deep learning in computer vision: A survey," *IEEE Access*, vol. 6, pp. 14410–14430, 2018.

YONG YANG received the master's degree in computer application technology from the China University of Mining and Technology in 2009. He is currently a Lecturer with the Xuzhou College of Industrial Technology. His research interests include signal processing, machine learning, and physical geography.

JIANHUA YUE received the Ph.D. degree in applied geophysics from the China University of Mining and Technology in 1997. He is currently a Professor with the China University of Mining and Technology. His research interests include physical geography and water bursting predictions in mines.

JING LI received the Ph.D. degree in communication and information system from Southeast University in 2017. He is currently a Lecturer with Nanjing Audit University. Her research interests include signal processing, sensor array technology as applied to rotating machinery fault diagnosis applications using AE technique.

ZHONG YANG received the Ph.D. degree from the Nanjing University of Aeronautics and Astronautics in 1996. He is currently a Professor with the Jinling Institute of Technology. His current interests concentrate on solar energy photovoltaic generating, building energy conservation, pattern recognition, and machine learning.